

MICROSTRUCTURE, TEXTURE AND MECHANICAL PROPERTIES OF A FRICTION-STIR-PROCESSED Mg-Al-Ca-Mn-Zn ALLOY

MIKROSTRUKTURA, TEKSTURA IN MEHANSKE LASTNOSTI TORNO-VRTILNO PROCESIRANE Mg-Al-Ca-Mn-Zn ZLITINE

Leipeng Song¹, Yang Zhang¹, Yalin Lu^{1,2*}, Xingcheng Li², Jian Wang¹,
Jiangtao Wang²

¹School of Materials Engineering, Jiangsu University of Technology, No. 1801 Zhongwu Road, Changzhou, Jiangsu 213001, China
²Key Laboratory of Advanced Materials Design and Additive Manufacturing of Jiangsu Province, No. 1801 Zhongwu Road, Changzhou, Jiangsu 213001, China

Prejem rokopisa – received: 2019-04-28; sprejem za objavo – accepted for publication: 2019-06-27

doi:10.17222/mit.2019.090

Microstructure, texture and mechanical properties of a friction-stir-processed (FSPed) Mg-1Al-0.3Ca-0.3Mn-0.6Zn (*w/w*) alloy were investigated in the present work. During FSP, complete dynamic recrystallization (DRX) takes place in the coarse primary α -Mg matrix and a considerable grain refinement is achieved. Furthermore, DRXed grain sizes increase with an increase of the rotation speed from 1000 min⁻¹ to 1600 min⁻¹, which is attributed to the integrated effect of the strain rate and thermal input. After FSP, a strong {0001} basal texture is formed, with the intensity ranging from 83.64 to 105.19. Compared to the base metal, the elongation is significantly enhanced, by $\approx 158\%$, while the ultimate tensile strength and yield strength are reduced. The variation in the mechanical properties is mainly due to the grain refinement and strong {0001} basal texture obtained with FSP.

Keywords: Mg-Al-Ca-Mn-Zn alloy, friction-stir processing, microstructure, texture

V članku avtorji opisujejo raziskave mikrostrukture, teksture in mehanskih lastnosti tornovrtilnega postopka (FSP) Mg-1Al-0,3Ca-0,3Mn-0,6Zn (v mas. %) zlitine. Med FSP-postopkom je prišlo do popolne dinamične rekristalizacije (DRX) v grobi primarni matrici α -Mg in do znatnega udrobljenja mikrostrukture. Nadalje se je velikost dinamično rekristaliziranih zrn povečala s povečanjem hitrosti vrtenja orodja iz 1000 min⁻¹ na 1600 min⁻¹, kar so pripisali celovitemu učinku hitrosti deformacije in vnosa toplote. Med izvedbo FSP-postopka je prišlo do tvorbe močne {0001} bazalne teksture, z intenziteto med 83,64 in 105,19. V primerjavi z osnovno zlitino je raztezek FSP-zlitine močno narasel (za približno 158 %), medtem ko sta se natezna trdnost in meja tečenja znižali oz. zmanjšali. Sprememba mehanskih lastnosti je predvsem posledica udrobljenja mikrostrukture in nastanka močne {0001} bazalne teksture zaradi izvedbe FSP-postopka.

Ključne besede: Mg-Al-Ca-Mn-Zn zlitina, tornovrtilni postopek varjenja, mikrostruktura, tekstura

1 INTRODUCTION

Magnesium alloys are recognized as environment-friendly materials with favorable properties including low density, high specific strength and stiffness, which make them fascinating candidates for applications in the fields of transportation and aerospace.^{1,2} Friction-stir processing (FSP) attracted much attention in the past decades.^{3,4} During FSP, dynamic recrystallization takes place in the nugget zone, leading to a significant grain refinement. The grain refinement plays the key role in enhancing the strength, which can be described with the Hall-Patch formula.^{5,6} According to the previous references, the majority of FSPed Mg alloys show a moderate increase in the strength, while a fraction of them exhibit diametrically opposite results.^{7,8} Besides the grain size, the texture was also found to have a significant influence on the comprehensive performance of wrought magnesium alloys.^{9,10} FSW leads to an enormous reduction in

the grain-boundary misorientation of AZ31 alloys due to the low symmetry of the hexagonal close-packed (HCP) structure and limitations of the {0001} texture.¹¹ And the role of the texture in deteriorating the yield strength (YS) of FSPed magnesium alloys was also investigated.¹²⁻¹³

T. Nakata et al.¹⁴⁻¹⁵ reported that a complex microalloyed Mg-1.3Al-0.3Ca-0.4Mn (*w/w*) alloy with merits of low cost shows favorable mechanical properties after an extrusion, and a further addition of the Zn element was beneficial to the mechanical properties. However, there has been limited investigation on the FSP of the Mg-Al-Ca-Mn-Zn alloy. In the present study, a Mg-1Al-0.3Ca-0.3Mn-0.6Zn (*w/w*) alloy was subjected to FSP with different rotational speeds. The purpose of the present study was to investigate the variations of the microstructure, texture and mechanical properties of the FSPed Mg-1Al-0.3Ca-0.3Mn-0.6Zn (*w/w*) alloy.

*Corresponding author's e-mail:
luyalin@163.com (Yalin Lu)

2 EXPERIMENTAL PART

The alloy selected for the present investigation was Mg-1Al-0.3Ca-0.3Mn-0.6Zn in *w/w%*, fabricated from high-purity Mg, Al, Zn (99.9 *w/w%*) and Mg-20 *w/w%*Ca, Mg-5 *w/w%* Mn master alloys using a vacuum induction furnace with an argon atmosphere. Plates with a thickness of 8 mm were cut from the ingots. Then solid-solution treatment was carried out at 410 °C for 24 h and followed by water quenching. The solid-solutioned base metal was designated as BM.

During FSP, a tool with a shoulder of 15 mm in diameter and a cylindrical screw pin of 4 mm in root diameter and 4 mm in length were utilized. The tool tilt angle was kept constant at 2.5° and the tool plunge depth was 5 mm. FSP was carried out at different rotational speeds (1000, 1300 and 1600) min⁻¹, while the travel speed was kept as 60 mm/min. Microstructure observation was conducted on the BM and FSPed alloy using an optical microscope (OM). The texture variation in the SZ of the FSPed alloy was examined using electron backscatter diffraction (EBSD). Tensile tests were implemented on a universal testing machine with a strain rate of 1×10⁻³ s⁻¹ along the processing direction. At least three specimens were processed for each condition to

obtain the mean values of mechanical properties. Tensile-fracture morphologies were examined using scanning electron microscopy (SEM).

3 RESULTS AND DISCUSSION

Figure 1 reveals the macrostructure of the transversal cross-section of an FSPed specimen. RS denotes the retreating side and AS denotes the advancing side. Based on macrostructural observations, the typical zones of an FSPed Mg alloy, including the stir zone (SZ), the thermo-mechanically affected zone (TMAZ) and BM are marked. Obvious boundaries between the violently stirred region and BM are observed, indicating the difference in the microstructure.

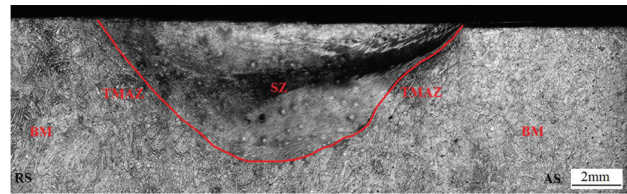


Figure 1: Cross-sectional macrostructure of an FSPed specimen

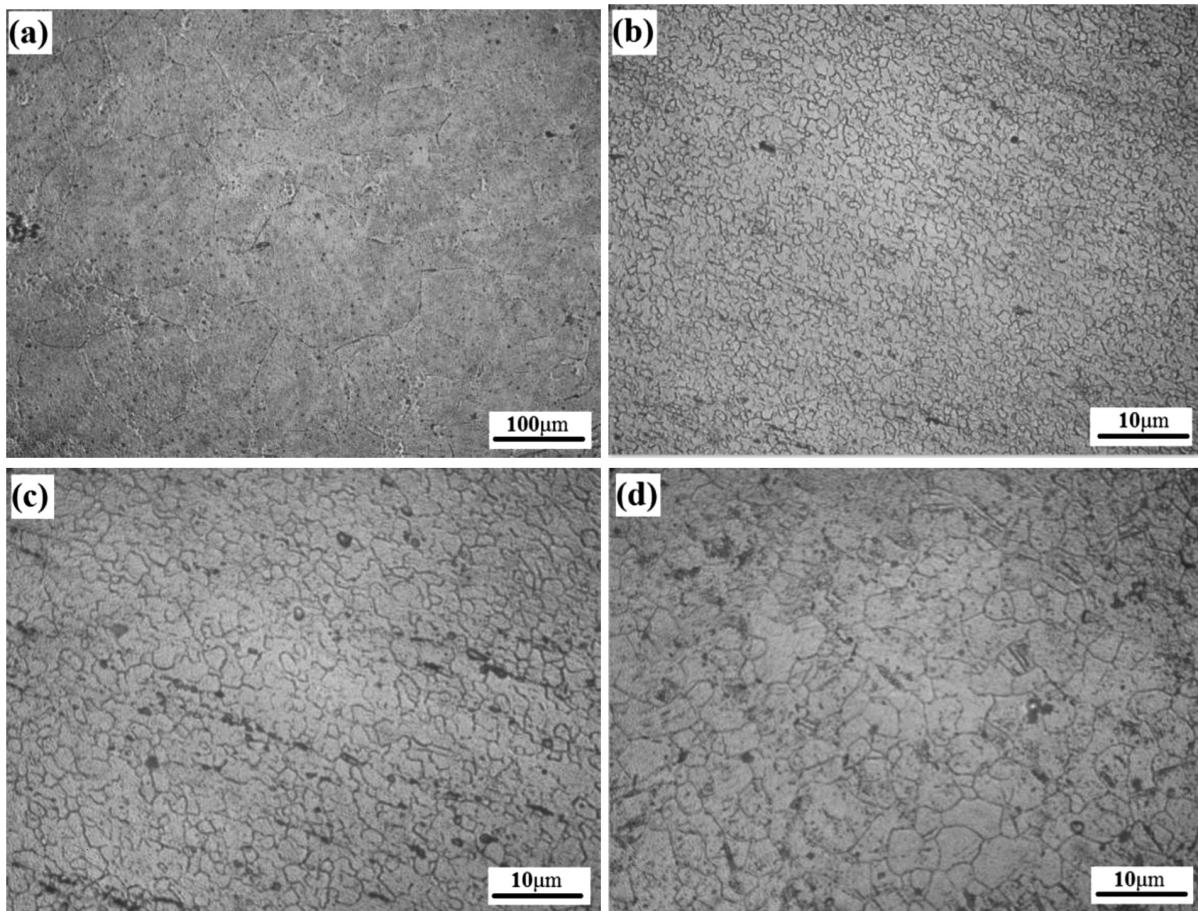


Figure 2: Microstructure of the BM and the central area of the SZ of the FSPed specimens at different rotational speeds: a) BM, b) 1000 min⁻¹, c) 1300 min⁻¹ and d) 1600 min⁻¹

Figure 2 shows the microstructure of the BM and the central area of the SZ of the FSPed specimens at different rotational speeds. As shown in **Figure 2a**, the BM contains coarse α -Mg grains with the mean grain size of $\sim 75 \mu\text{m}$. After FSP, a complete DRX took place in the coarse primary α -Mg matrix and fine equiaxed grains were obtained. Compared to the BM, the grains of the FSPed specimens became considerably refined. A quantitative analysis of the DRXed grain size was conducted following the EBSD analysis.

Figure 3 shows the inverse pole-figure maps of the FSPed specimens at different rotational speeds obtained with EBSD. Black lines represent high-angle grain bound-

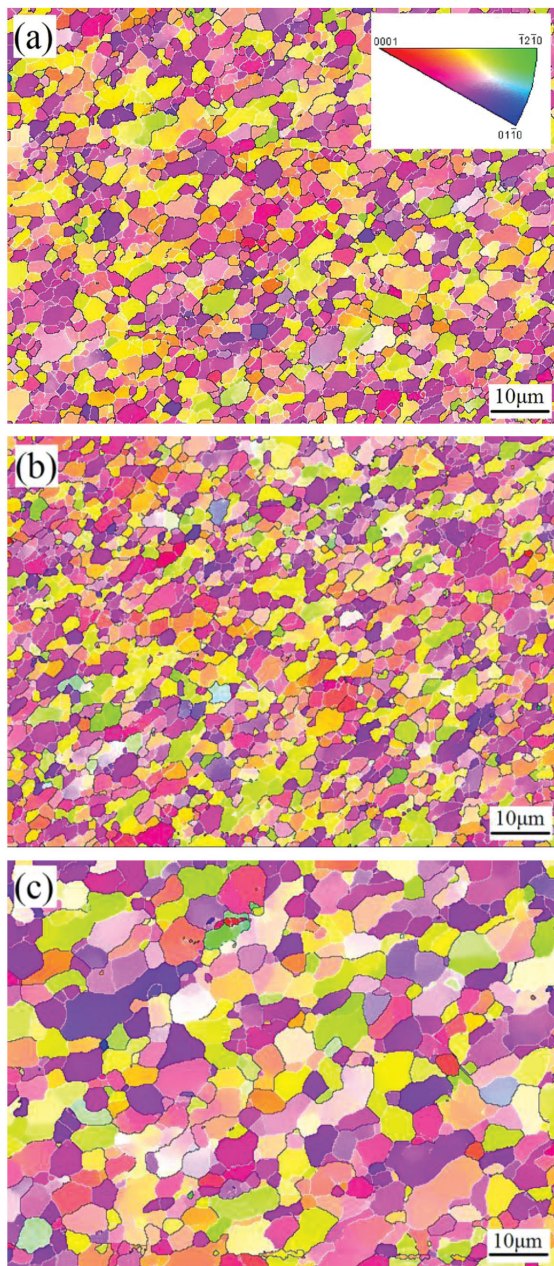


Figure 3: Inverse pole-figure maps of the FSPed specimens at different rotational speeds: a) 1000 min^{-1} , b) 1300 min^{-1} , c) 1600 min^{-1}

aries (HAGB) with a misorientation angle larger than 15° and white lines represent low-angle grain boundaries (LAGB) with a misorientation angle smaller than 15° but larger than 2° . The EBSD analysis also confirmed that a complete DRX took place in these specimens and the DRXed grain size increased with an increase of the rotational speed from 1000 min^{-1} to 1600 min^{-1} . The mean grain sizes of the FSPed alloy were $2.64 \mu\text{m}$ for 1000 min^{-1} , $3.22 \mu\text{m}$ for 1300 r/min , and $5.20 \mu\text{m}$ for 1600 min^{-1} . In addition, the rotation of the DRXed grains took place during FSP, showing a visibly preferential orientation. DRX during FSP is promoted by the thermo-mechanical effect. The strain rate during FSP is greatly related to the rotational speed.¹⁶ Besides the strain rate, the thermal input also has a significant influence on the microstructure evolution during FSP.¹⁷ When the feed speed is kept constant, the increased rotational speed is accompanied by a great thermal input, which can induce a coarsening of DRXed grains. Therefore, the variation in the microstructure is the interactional outcome of the strain rate and thermal input.

Figure 4 shows the $\{0001\}$ pole figures of the FSPed specimens at different rotational speeds, where ND, PD and TD denote the normal direction, the processing direction and the transverse direction, respectively. As shown in **Figure 4**, a strong $\{0001\}$ basal texture is formed in the FSPed specimens, with the texture intensity ranging from 83.64 to 105.19.

Figure 5 shows the effect of the rotational speed on the tensile properties of the FSPed specimens and **Table 1** exhibits detailed data of the tensile properties. The ultimate tensile strength (UTS), yield strength (YS) and elongation (EL) of the BM are 164 MPa, 82 MPa and 14.3 %, respectively. As shown in **Figure 5**, the strain-stress curve of the BM shows slip characteristics

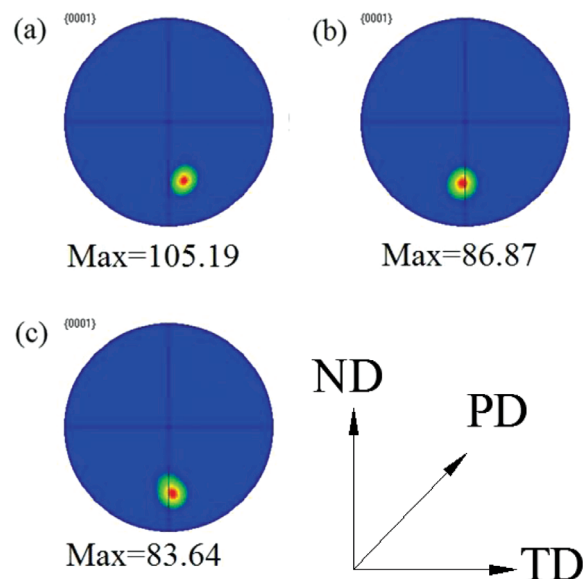


Figure 4: Pole figures of the FSPed specimens at different rotational speeds: a) 1000 min^{-1} , b) 1300 min^{-1} , c) 1600 min^{-1}

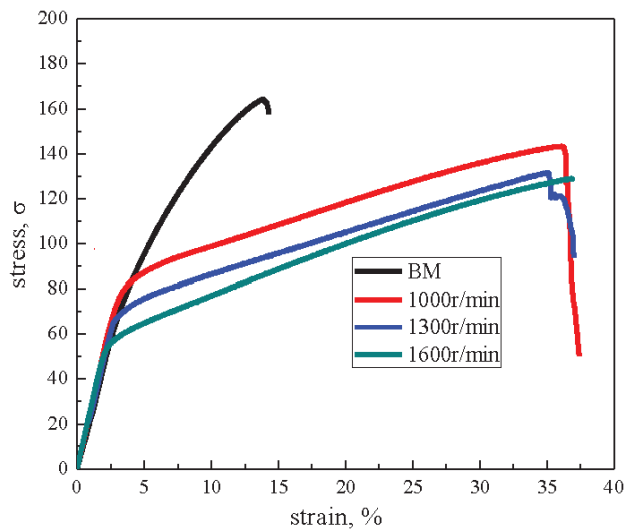


Figure 5: Effect of rotational speed on the tensile properties of FSPed specimens

at a high YS and low EL, attributed to the initial grain orientation with a low Schmid factor for the basal slip or extension twinning. After FSP, the EL of the specimens increases dramatically, by $\approx 158\%$. On the other hand, the YS has a different rate reduction, especially at 1600 min^{-1} . The YS at 1600 min^{-1} decreases by 40% in comparison with the BM. The UTS of the FSPed specimens is also on the decline. However, the UTS and YS

of the FSPed specimens decrease with an increase in the rotational speed.

Table 1: Tensile properties of BM and FSPed specimens at different rotational speeds

Specimens	UTS / MPa	YS / MPa	Elongation / %
BM	164	82	14.3
FSP-1000 min^{-1}	143	79	37.4
FSP-1300 min^{-1}	133	67	37.0
FSP-1600 min^{-1}	129	53	36.8

Figure 6 shows SEM images of the tensile-fracture morphologies. As shown in **Figure 6a**), the tensile fracture of the BM is characterized by a typical intergranular fracture including a cleavage fracture (indicated by a white arrow) and a large hollow (surrounded by a black frame) due to the separation of coarse grains. The orientation of the cleavage plane is related to the angle between the grain and the tensile axis. It can be seen in **Figure 6b** to **6d**) that the FSP fracture surface is much flatter than the BM fracture surface, characterized by a fine grain fracture due to the unidirectional crack propagation along the banded structure.

As shown in **Figure 5** and **Table 1**, the application of FSP to the Mg-1Al-0.3Ca-0.3Mn-0.6Zn (*w/w%*) alloy leads to an increase in the EL of about 158% in comparison to the BM. As shown in **Figure 2**, compared to the BM, the grain sizes of the FSPed alloys are considerably

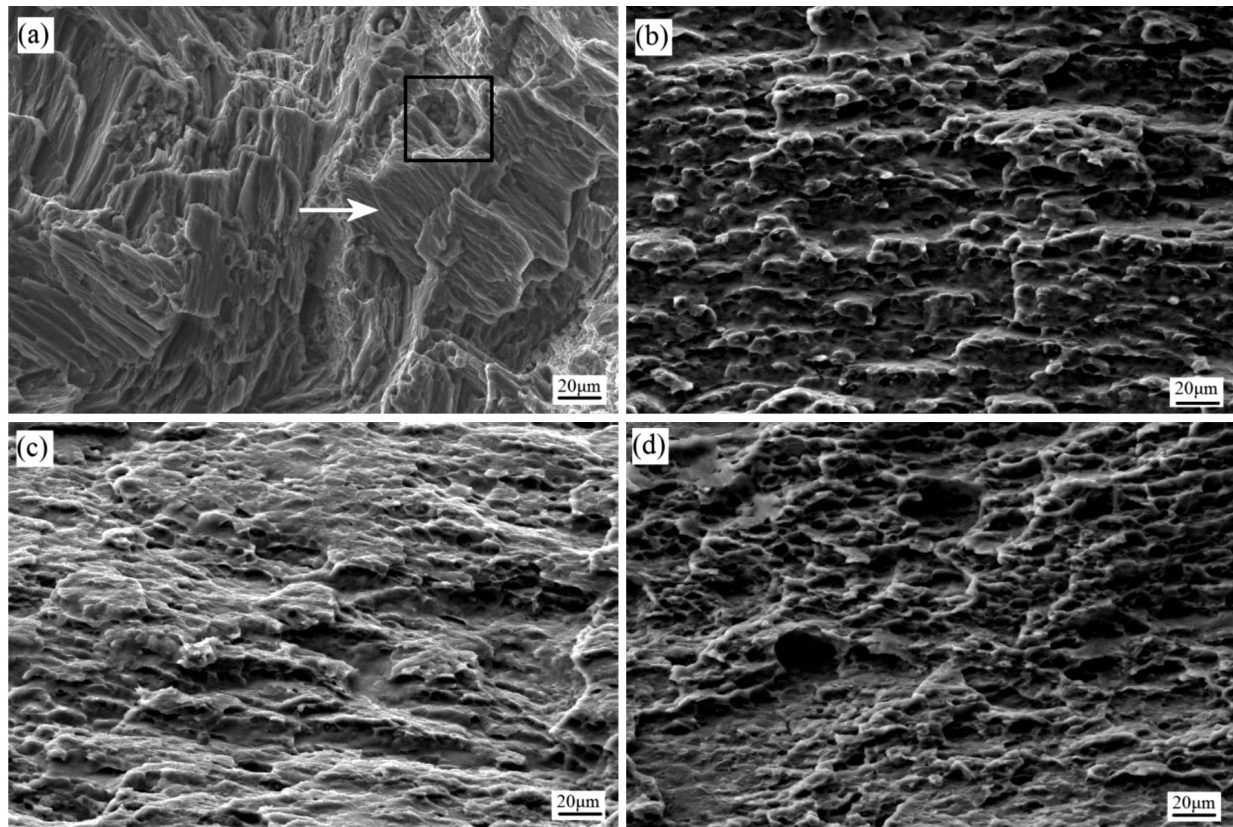


Figure 6: SEM images of the tensile-fracture morphologies: a) BM, b) 1000 min^{-1} , c) 1300 min^{-1} and d) 1600 min^{-1}

refined. It is well accepted that the grain refinement can activate non-basal slipping in magnesium alloys, which can enhance the plastic deformability, and then the EL increases accordingly. More importantly, the pole figures from **Figure 4** show that after FSP, the FSPed alloy exhibits an extremely strong {0001} basal texture. The observed strong distinction in the intensity of texture components suggests that the dominant plastic deformation mode is the <a> slip, while the deformation in the <c> direction is minor. It is also reported that a texture modification significantly improves the EL of magnesium alloys due to the formation of a strong {0001} basal texture, moving the easy basal-slip system to the preferred orientation.¹⁸ A similar report on a texture causing an improvement of the ductility was provided by M. Vargas.¹⁹

However, the strength of the BM declines after FSP, which is not consistent with the Hall-Petch formula. A previous study of FSPed AZ31 suggested that soft orientation was the main reason of this phenomenon.²⁰ W. Yuan et al.²¹ pointed out that the texture would affect the Hall-Petch relationship since soft orientation of a basal texture would cause a decrease in the strength, while hard orientation of a basal texture would make it difficult for the basal slip system to become activated. During FSP, a complete DRX and simultaneous grain rotation contribute to the soft orientation of the basal texture, causing a decrease in the UTS and YS. Moreover, a strong {0001} texture can also weaken the work-hardening ability and result in a low UTS (**Figure 5**). Therefore, the effect of grain refinement on the strength is counteracted by the effect of the texture in some FSPed samples. However, as for FSPed alloys, since the effect of the texture on the strength is almost the same in this study, the difference in the grain size shows an obvious influence on the YS of FSPed specimens and the FSPed specimen at 1600 min⁻¹ with the largest grain size exhibits the lowest YS among the FSPed specimens.

4 CONCLUSIONS

In this study, the microstructure, texture and mechanical properties of an Mg-1Al-0.3Ca-0.3Mn-0.6Zn alloy after FSP are systematically investigated. The main conclusions are as follows:

1) During FSP, a complete DRX takes place in the coarse primary α -Mg matrix and a considerable microstructural refinement is achieved. DRXed grain sizes increase with an increase of the rotational speed from 1000 min⁻¹ to 1600 min⁻¹, which is attributed to the interactional outcome of the strain rate and thermal input.

2) After FSP, a strong {0001} basal texture is formed in the FSPed specimens, with the texture intensity ranging from 83.64 to 105.19. The texture intensity peaks of {0001} turn by approximately 30° from the ND towards the PD.

3) The EL of the FSPed specimens is significantly enhanced, by $\approx 158\%$, while the YS and UTS are reduced. The variation in the mechanical properties is due to the grain refinement and strong {0001} basal texture obtained with FSP.

Acknowledgment

This research was funded by the National Natural Science Foundation of China (No. 51601076), Major Project of the Natural Science Foundation from the Jiangsu Higher Education Institutions (no. 17KJA430005, No. 18KJA430007), the Natural Science Foundation of the Jiangsu Higher Education Institutions (No. 16KJB430013) and Postgraduate Research & Practice Innovation Program of the Jiangsu Province (No. SJCX18_1043).

5 REFERENCES

- A. Y. Zhang, R. Kang, H. C. Pan, L. Wu, H. C. Pan, H. B. Xie, Q. Y. Huang, Y. J. Liu, Z. R. Ai, L. F. Ma, Y. P. Ren, G. W. Qin, A new rare-earth-free Mg-Sn-Ca-Mn wrought alloy with ultra-high strength and good ductility, *Mater. Sci. Eng. A*, 754 (2019), 269–274, doi:10.1016/j.msea.2019.03.095
- Y. F. Wang, F. Zhang, Y. T. Wang, Y. B. Duan, K. J. Wang, W. J. Zhang, J. Hu, Effect of Zn content on the microstructure and mechanical properties of Mg-Gd-Y-Zr alloys, *Mater. Sci. Eng. A*, 745 (2019), 149–158, doi:10.1016/j.msea.2018.12.088
- I. Charit, R. S. Mishra, Effect of friction stir processed microstructure on tensile properties of an Al-Zn-Mg-Sc alloy upon subsequent aging heat treatment, *J. Mater. Sci. Technol.*, 34 (2018), 214–218, doi:10.1016/j.jmst.2017.10.021
- Y. Y. Jin, K. S. Wang, W. Wang, P. Peng, S. Zhou, L. Y. Huang, T. Yang, K. Qiao, B. Zhang, J. Cai, H. L. Yu, Microstructure and mechanical properties of AE42 rare earth-containing magnesium alloy prepared by friction stir processing, *Mater. Charact.*, 150 (2019), 52–61, doi:10.1016/j.matchar.2019.02.008
- Y. L. Lu, Y. Zhang, M. Q. Cong, X. C. Li, W. T. Xu, L. P. Song, Microstructure and mechanical properties of extruded AZ31-xCaO alloy, *Materials*, 11 (2018), 1–14, doi:10.3390/ma11081467
- Y. Zhang, L. P. Song, X. Y. Chen, X. P. Li, Effect of Zn and Ca addition on microstructure and strength at room temperature of as-cast and as-extruded Mg-Sn alloy, *Materials*, 11 (2018), 1–14, doi:10.3390/ma11091490
- Y. X. Huang, Y. B. Wang, X. C. Meng, L. Wan, J. Cao, L. Zhou, J. C. Feng, Dynamic recrystallization and mechanical properties of friction stir processed Mg-Zn-Y-Zr alloys, *J. Mater. Process. Technol.*, 248 (2017), 331–338, doi:10.1016/j.jmatprotec.2017.06.021
- F. Khan MD, G. M. Karthik, S. K. Panigrahi, G. D. Janaki, Friction stir processing of QE22 magnesium alloy to achieve ultrafine-grained microstructure with enhanced room temperature ductility and texture weakening, *Mater. Charact.*, 147 (2019), 365–378, doi:10.1016/j.matchar.2018.11.020
- Q. Shang, D. R. Ni, P. Xue, B. L. Xiao, K. S. Wang, Z. Y. Ma, An approach to enhancement of Mg alloy joint performance by additional pass of friction stir processing, *J. Mater. Process. Technol.*, 264 (2019), 336–345, doi:10.1016/j.jmatprotec.2018.09.021
- N. Xu, Q. N. Song, Y. F. Bao, {10-12} twinning assisted microstructure and mechanical properties modification of high-force friction stir processed AZ31B Mg alloy, *Mater. Sci. Eng. A*, 745 (2019) 4, 400–403, doi:10.1016/j.msea.2018.12.127

- ¹¹ S. Mironov, T. Onuma, Y. S. Sato, H. Kokawa, Microstructure evolution during friction-stir welding of AZ31 magnesium alloy, *Acta Mater.*, 100 (2015), 301–312, doi:10.1016/j.actmat.2015.08.066
- ¹² S. H. Chowdhury, D. L. Chen, S. D. Bhole, X. Cao, P. Wanjara, Friction stir welded AZ31 magnesium alloy: microstructure, texture, and tensile properties, *Metall. Mater. Trans. A.*, 44 (2013) 1, 323–336, doi:10.1007/s11661-012-1382-3
- ¹³ R. L. Xin, B. Li, A. L. Liao, Z. Zhou, Q. Liu, Correlation between texture variation and transverse tensile behavior of friction-stir-processed AZ31 Mg alloy, *Metall. Mater. Trans. A*, 43 (2012) 7, 2500–2508, doi:10.1007/s11661-012-1080-1
- ¹⁴ T. Nakata, C. Xu, R. Ajima, K. Shimizu, S. Hanaki, T. T. Sasaki, L. Ma, K. Hono, S. Kamado, Strong and ductile age-hardening Mg-Al-Ca-Mn alloy that can be extruded as fast as aluminum alloys, *Acta Mater.*, 130 (2017), 261–270, doi:10.1016/j.actmat.2017.03.046
- ¹⁵ M. Z. Bian, T. T. Sasaki, B. C. Suh, T. Nakata, S. Kamado, K. Hono, A heat-treatable Mg-Al-Ca-Mn-Zn sheet alloy with good room temperature formability, *Scr. Mater.*, 138 (2017), 151–155, doi:10.1016/j.scriptamat.2017.05.034
- ¹⁶ C. I. Chang, C. J. Lee, J. C. Huang, Relationship between grain size and Zener-Holloman parameter during friction stir processing in AZ31 Mg alloys, *Scr. Mater.*, 51 (2004) 6, 509–514, doi:10.1016/j.scriptamat.2004.05.043
- ¹⁷ M. Abbasi Gharacheh, A. H. Kokabi, G. H. Daneshi, B. Shalchi, R. Sarrafi, The influence of the ratio of "rotational speed/traverse speed" (ω/v) on mechanical properties of AZ31 friction stir welds, *Int. J. Mach. Tools. Manuf.*, 46 (2006) 15, 1983–1987, doi:10.1016/j.ijmachtools.2006.01.007
- ¹⁸ W. Yuan, R. S. Mishra, Grain size and texture effect on deformation behavior of AZ31 magnesium alloy, *Mater. Sci. Eng. A*, 558 (2012), 716–724, doi:10.1016/j.msea.2012.08.080
- ¹⁹ M. Vargas, S. Lathabai, P. J. Uggowitzer, Y. Qi, D. Orlov, Y. Estrin, Microstructure, crystallographic texture and mechanical behaviour of friction stir processed Mg-Zn-Ca-Zr alloy ZKX50, *Mater. Sci. Eng. A*, 685 (2017), 253–264, doi:10.1016/j.msea.2016.12.125
- ²⁰ F. Y. Hung, C. C. Shih, L. H. Chen, T. S. Lui, Microstructures and high temperature mechanical properties of friction stirred AZ31–Mg alloy, *J. Alloy. Compd.*, 428 (2007) 1–2, 106–144, doi:10.1016/j.jallcom.2006.03.033
- ²¹ W. Yuan, R. S. Mishra, B. Carlson, R. K. Mishra, R. Verma, R. Kubic, Effect of texture on the mechanical behavior of ultrafine grained magnesium alloy, *Scr. Mater.*, 64 (2011) 6, 580–583, doi:10.1016/j.scriptamat.2010.11.052